Polymer Journal (2011) 43, 991–999

www.nature.com/pj

ORIGINAL ARTICLE

High performance reactive blends composed of poly(*p*-phenylene sulfide) and ethylene copolymers

Hideko T Oyama, Mayu Matsushita and Motonobu Furuta

Poly(*p*-phenylene sulfide) (PPS) is a high performance polymer that has superior chemical resistance and heat stability, but its brittleness is a serious drawback for applications. The objective of this work is to improve the physical properties of PPS by incorporating a small amount of either poly(ethylene-*ran*-methylacrylate–*ran*-glycidyl methacrylate) (EMA–GMA) or poly(ethylene-*ran*-glycidyl methacrylate)-*graft*-poly(methyl methacrylate) (EGMA-*g*-PMMA) by melt mixing under a high shear rate. It was demonstrated that the chemical reaction between PPS and EMA–GMA (or EGMA-*g*-PMMA) proceeded efficiently at the interface and that the domains of EMA–GMA (or EGMA-*g*-PMMA) were finely dispersed in the PSS matrix with size of ca 0.1–0.3 μm. The resultant copolymers formed at the interface contributed to a decrease in the interfacial tension and an increase in the interfacial adhesion so that the obtained PPS/EMA–GMA blends (or PPS/EGMA-*g*-PMMA blends) showed excellent mechanical properties, at the same time retaining high thermal stability.
Polymer Journal (2011) **43,** 991–999; doi:10.1038/pj.2011.106; published online 19 October 2011

Keywords: blend; copolymer; interface; poly(ethylene-*ran*-glycidyl methacrylate); poly(phenylene sulfide)

INTRODUCTION

Poly(phenylene sulfide) (PPS) is a high performance super-engineering plastic with high thermal stability (over 150 °C), excellent chemical resistance (no solvents under 200 °C), good electrical and electronic properties, good mold precision, and high stiffness and modulus (tensile modulus=2600–3900 MPa).[1] The semi-crystalline PPS has a T_g of 88–93 °C, T_m of 280–285 °C and an equilibrium melting point of its orthorhombic crystals at 303–350 °C.[1–3] Furthermore, PPS shows extraordinary flame retardance, having a limited oxygen index of 44%, which belongs to the highest group among polymeric materials together with poly(vinyl chloride) and polyimide.[4] So taking advantage of these unique properties, PPS has been applied as an alternative material for metals and thermoset polymers; for example, automobile parts and electrical and electronics parts.[1] However, its low toughness and high brittleness, which originate from its rigid structure, are serious drawbacks, preventing further applications.

Thus, in order to improve the properties of PPS, blending of PPS has been intensively studied, and can be categorized into three groups. The first group of PPS blends are formed with other high performance super-engineering plastics, such as polysulfone,[5] poly(ether sulfone) (PES)[6,7] and liquid crystalline polymers (LCPs),[8–10] which have thermal stability over 150 °C for long durations. It is reported that PPS blends having an amorphous polysulfone matrix ($\leqslant$50 wt% of PPS) show good tensile properties, but that blends having a PPS matrix ($>$50 wt% of PPS) become brittle.[5] It was found that PPS and PES are partially miscible, in which PES is also an amorphous polymer having excellent mechanical properties.[6] Although mechanical properties are not reported in the same paper, it was found that the activation energy of crystallization of PPS increases by blending with PES and that the equilibrium melting temperature decreases linearly with increase of the PES content. Furthermore, in another study on PPS blends with thermotropic LCP, it is reported that the LCP initially dispersed as spheres or droplets was elongated in adequate flow fields to give an *in situ* matrix reinforcement.[9] However, most blends composed of thermoplastic polymers such as PPS and thermotropic LCPs show very poor interfacial adhesion resulting in inferior mechanical properties. So in the same paper, it was also attempted to add dicarboxyl-terminated PPS when conventional PPS and LCP are blended, in which the interfacial reaction between the carboxyl end-group of the modified PPS and the ester linkages of LCP results in block copolymers via transesterification. It was demonstrated that the so-compatibilized interface in PPS/LCP blends significantly contributes to the enhancement of tensile properties and impact strength.[10]

The second group of PPS blends is formed with conventional engineering plastics with thermal stability between 100–140 °C for long usage such as crystalline polyamide (PA)[11–13] and poly(ethylene terephthalate) (PET),[14–16] and amorphous poly(phenylene ether)[17] and polycarbonate (PC).[18] It is reported that (20/80) PPS/PA4,6 (T_m of PA4,6=295 °C) blends have a miscible region, which appears under a high shear rate at 310–320 °C[13] although the solubility parameter of PPS is extremely high (12.5 (cal cm^{-3})$^{0.5}$) compared with other polymers and this makes it difficult for PPS to have miscibility with other polymers.[19] Among various studies on PPS/PA

Department of Chemistry, College of Science, Rikkyo University, Tokyo, Japan
Correspondence: Professor HT Oyama, Department of Chemistry, College of Science, Rikkyo University, 3-34-1 Nishi-Ikebukuro, Toshima-ku, Tokyo 171-8501, Japan.
E-mail: hideko-oyama@rikkyo.ac.jp
Received 7 July 2011; revised and accepted 12 September 2011; published online 19 October 2011

blends, PA66 is the most intensively investigated because of its superior mechanical properties, especially when exposed to solvents at elevated temperatures.[11,12,19] It was observed that the Izod impact strength and elongation at break of the PPS/PA66 are increased by moisture uptake.[19] This binary PPS/PA66 system has been further developed into ternary systems by the addition of another component such as a compatibilizer to efficiently improve mechanical properties,[11,12] an internal lubricant poly(tetrafluoroethylene) to increase the wear resistance,[20] glass fiber[21] and carbon nanotubes[22] to reinforce the polymer matrix. Furthermore, in a study of PPS/PET blends in the presence of pre-made PPS-*graft*-PET copolymer it was found that the presence of the PPS matrix increased the crystallization temperature of PET domains, in which the magnitude of the increase in the PET crystallization temperature coincided with the viscosity ratio and the extent of solubilization of PPS homopolymer into the graft copolymer.[15] In PPS/PC blends, as inherently high interfacial tension would result in an unstable interface,[23] a small amount of epoxy resin was added to the PPS/PC blends. In this system it is surmised that the epoxy resin reacts with the hydroxyl group located at the PC chain ends, which is generated by hydrolysis of PC during melt blending.[18] It was demonstrated that the tensile strength and tensile modulus of PPS/PC blends were significantly increased upon the addition of epoxy resin.

The third group is PPS blends prepared with general-purpose polymers, which have lower thermal stability; for example, polyethylene,[24] elastomers,[25] polystyrene,[26] and reactive ethylene copolymers.[27,28] Studies in this group are very limited compared with the other two groups, because it is believed that the general-purpose polymers cannot tolerate the high temperature process required for blending with PPS. Chen *et al.*[24] studied blends composed of PPS and polyethylene at various component ratios and described the relationship between the domain size and the composition. It was observed that the cryogenically fractured surface of polyethylene domains in the PPS matrix showed protruding fibrils and that of PPS domains in the polyethylene matrix had an orange-peel appearance, which was probably caused by the sequential crystallization of the two phases and the loose packing of PPS crystallites in the intermediate stage of solidification.[24] It was further attempted to reduce the brittleness of PPS by blending with polystyrene-*block*-poly(ethylene-butylene)-*block*-polystyrene copolymers (SEBS) containing maleic anhydride groups.[25] It was found that in the resultant PPS alloys with SEBS, highly modified with maleic anhydride, the toughness was improved by void formation in the SEBS particles, which efficiently released constraint of the strain. By contrast, in the PPS alloys with unmodified or lightly modified SEBS with maleic anhydride the diameter of the dispersed SEBS domains was larger and the domains deformed into rod-like shapes that were oriented along to the direction of injection flow and were easily fractured, thereby suppressing improvement of the toughness of the alloy.

It was also attempted to form PPS blends with reactive ethylene copolymers. For example, Masamoto *et al.*[27] first reacted PPS with a diisocyanate derivative and then blended the so-modified PPS with ethylene copolymer containing ca 2 wt% of maleic anhydride. They reported that energy dissipation by matrix yielding enhances the notched Izod impact strength of the (80/20) PPS/ethylene copolymer by 50 times compared with that of pristine PPS. Moreover, the critical surface-to-surface interparticle distance, under which the impact strength is drastically increased, was located at about 0.1 μm for the PPS alloys. Furthermore, another PPS alloy with poly(ethylene-*stat*-glycidyl methacrylate)-*graft*-poly(acrylonitrile-*stat*-styrene) was prepared and its mechanical properties were investigated at −50, 25 and 150 °C.[28] The results of these works will be compared in detail with our results later.

In this study, first, a difference between reactive blends of PPS, that is, PPS/poly(ethylene-*ran*-methylacrylate–*ran*-glycidyl methacrylate) (EMA–GMA) and PPS/poly(ethylene-*ran*-glycidyl methacrylate)-*graft*-poly(methyl methacrylate) (EGMA-*g*-PMMA), and a non-reactive blend of PPS/linear low-density polyethylene (LDPE) prepared at high shear rate is elucidated from the viewpoints of melt viscosity and morphology. Then, the mechanical properties and the thermal stability are shown for the reactive PPS blends in comparison to pristine PPS and a non-reactive PPS blend, and the results are also compared with those of other PPS blends reported in the literature.

EXPERIMENTAL PROCEDURE

Materials

Poly(*p*-phenylene sulfide) (PPS) was obtained from Toray Industries, Inc. (Tokyo, Japan, grade name of Torelina A900) and its density was reported to be 1.342 $cm^3\,g^{-1}$. EMA–GMA containing 30 wt% of methylacrylate and 3 wt% of GMA was supplied from Sumitomo Chemical Co. (Tokyo, Japan, grade name of Bondfast 7L). Its number-average (M_n) and weight-average (M_w) molecular weights estimated by gel permeation chromatography in our laboratory were 4.7×10^4 and 18.7×10^4 g mol^{-1}, respectively. EGMA-*g*-PMMA was obtained from NOF Co. (Tokyo, Japan, grade: Modiper A4200), which contains GMA, MMA and ethylene units to be 10.5 wt%, 30 wt%, and 59.5 wt%, respectively. It is reported that this EGMA-*g*-PMMA was synthesized by graft polymerization of PMMA to the EGMA main chain in a reactor. LDPE (grade name of Ultzex 20100J) was obtained from Prime Polymer Co. Ltd. (Tokyo, Japan). It is reported by manufacturers that the melt flow rate of EMA–GMA, EGMA-*g*-PMMA and LDPE are 7, 0.1 and 8.5 g per 10 min at 190 °C under 2.16 kg load, respectively, and that density of these polymers are 0.964, 0.993, and 0.916 g cm^{-3}, respectively.

Figure 1 shows the chemical structures of PPS, EMA–GMA, EGMA-*g*-PMMA and LDPE used in the present study. Table 1 summarizes the glass transition temperature (T_g) and melting point (T_m) of each specimen, which were estimated by differential scanning calorimetry (DSC) under the conditions mentioned in the section of 'Thermal analysis'. DSC analysis demonstrated that all ethylene copolymers have low T_g similar to LDPE and that incorporation of 30 wt% methylacrylate unit and 3 wt% GMA unit to the polyethylene backbone did not totally deprive the polyethylene units of the ability of crystallization, however, it significantly decreases crystallinity and T_m of EMA–GMA. This might imply that the actual distribution of the GMA and MMA groups in the polyethylene backbone is not necessarily random.

Melt mixing and compression-molded film formation

Before melt mixing, PPS were dried at 130 °C and EMA–GMA, EGMA-*g*-PMMA and LDPE were dried at room temperature *in vacuo* overnight. The polymers at given compositions were melt mixed in a twin blade mixer consisting of a motor and controller (Toyo Seiki, Labo Plastomill 4M150, manufactured in Tokyo, Japan) attached to a mixer (Toyo Seiki, KF70V2 manufactured in Tokyo, Japan) at 300 °C with a rotation speed of 100 rpm. To study the change in melt viscosity or morphology of the blend specimens during melt mixing, the effects of different mixing times were also investigated, however, most of the blends were prepared by melt mixing for 10 min unless otherwise stated.

This batch type mixer newly designed so as to give a high shear rate of molten polymers has the following dimensions: internal volume of 70 cc, cylinder inner diameter of 47.7 mm, respective disk long and short axis diameters of 46.9 and 29.3 mm, and clearance between the disk and the wall of 0.4 mm.

It is known that the shear rate (S) in melt mixing can be calculated according to the following equation:[29]

$$S = \pi \cdot D_m \cdot N/h \qquad (1)$$

where N=number of screw rotation per s, h=clearance between the disc and the wall surface of the mixer and D_m=the difference between the inner diameter of the cylinder and the long axis diameter of a disc. The shear rate

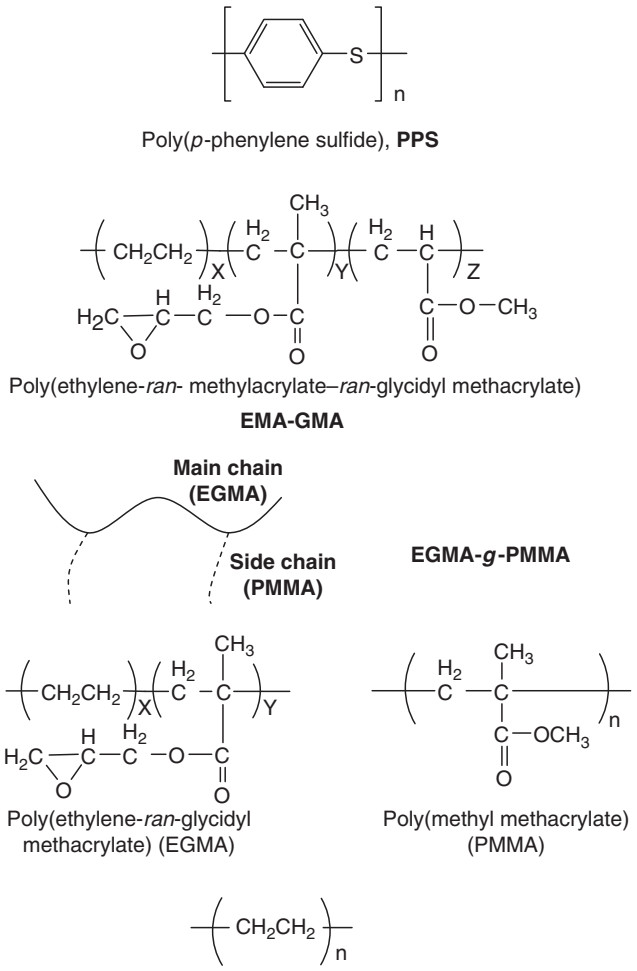

Figure 1 Chemical structures of poly(*p*-phenylene sulfide) (PPS), poly (ethylene-*ran*-methylacrylate–*ran*-glycidyl methacrylate) (EMA–GMA), poly (ethylene-*ran*-glycidyl methacrylate)-*graft*-poly(methyl methacrylate) (EGMA-*g*-PMMA) and linear low-density polyethylene (LDPE).

Table 1 Thermal properties of PPS, EMA–GMA, EGMA-*g*-PMMA and LDPE

	Thermal properties[a]	
	T_g (°C)	T_m (°C)
PPS	85	278
EMA–GMA	−33	68
EGMA-*g*-PMMA	−29	94
LDPE	−29	124

Abbreviations: EMA–GMA, poly(ethylene-*ran*-methylacrylate–*ran*-glycidyl methacrylate); EGMA-*g*-PMMA, poly(ethylene-*ran*-glycidyl methacrylate)-*graft*-poly(methyl methacrylate); PPS, poly(*p*-phenylene sulfide); LDPE, linear low-density polyethylene; T_g, glass transition temperature; T_m, melting point.
[a]Differential scanning calorimetry measurements were carried out at a heating rate of 10 °C per min under a N_2 atmosphere. T_g and T_m were determined from their heat flow curves.

of the mixer (S) in this study is estimated to be 1.2×10^3 (s^{-1}) at the highest from equation (1), indicating that the PPS blends in the present study were prepared under very high shear rate. The resultant blends were first hot-pressed at 310 °C under 20 MPa for 5 min and then quickly cold-pressed at 20 °C to prepare films with ca 500 μm thickness.

Structural analysis

The morphology of the melt-mixed materials was investigated by transmission electron microscopy (TEM), in which samples exposed to RuO_4 vapor were microtomed at room temperature before the measurements. A JEM1230 TEM instrument manufactured by JEOL in Japan was used with an acceleration voltage of 120 kV.

Mechanical tests

All mechanical tests were repeated at least five times using film specimens with ca 500 μm thickness. Tensile properties and tensile impact tests were performed at room temperature following the ISO 527 and 8256 procedures, respectively, of which details were described in our previous paper.[30] In the tensile impact tests, one end of a film specimen with dumbbell shape is mounted on a stationary stage and the other end is clipped with a crosshead bar; and when the specimen is broken as a result of striking the crosshead bar by a pendulum, energy of the specimen failure is measured as tensile impact strength.

Thermal analysis

DSC was carried out to estimate the glass transition temperature (T_g) and melting point (T_m) of specimens under a nitrogen atmosphere with a differential scanning calorimeter (TA Instruments, DSC-Q200, manufactured at New Castle, DE, USA) at a heating rate of 10 °C per min. Thermogravimetric analysis was performed on a TA Instruments TGA-Q50 manufactured in the USA at a heating rate of 5 °C per min from room temperature to 500 or 600 °C under a nitrogen atmosphere.

Melt viscosity

In the present study, the apparent melt viscosity of component polymers and the blends was measured separately using a plunger-type capillary rheometer, Capillograph E3B type (L/D=10/1) manufactured by Toyo Seiki, Japan, at 300 °C by changing the flow rate. In this measurement the apparent shear rate (γ_a) is estimated by the following equation,[31]

$$\gamma_a = \frac{4Q}{\pi r^3} \tag{2}$$

where Q and r are the flow rate and the radius of the capillary in the apparatus. Results were compared at a flow rate of 100 mm min^{-1}, which corresponds to $\gamma_a=1.260\times10^3$ (s^{-1}), very close to the maximum shear rate used for the sample preparation.

RESULTS AND DISCUSSION

Morphology of PPS/EMA–GMA, PPS/EGMA-*g*-PMMA and PPS/LDPE

In Figure 2, the apparent melt viscosity of the PPS/EMA–GMA (or PPS/LDPE) blends at different mixing times is shown with that of their component polymers. The apparent melt viscosity of (80/20) PPS/EMA–GMA at different mixing times measured at the flow speed of 100 mm min^{-1} is shown as (d), in which the flow rate approximately corresponds to the maximum shear rate used for the sample preparation. It was found that the apparent melt viscosity of PPS/EMA–GMA became lower at 2 min of mixing time compared with that of pristine PPS (a). However, it increased drastically at 10 min and stayed constant at 20 min, at a value exceeding that of pristine PPS. Similar results were also observed in PPS/EGMA-*g*-PMMA, although the data are not included in Figure 2: the apparent melt viscosity of PPS/EGMA-*g*-PMMA at 10 min of mixing time became higher (387 (Pa s^{-1})) when compared with that for pristine PPS (283 (Pa s)). By contrast, the apparent melt viscosity of PPS/LDPE (e) stayed much lower than that of pristine PPS at both 2 and 10 min of mixing time. These results clearly indicate that PPS reacts with EMA–GMA (or EGMA-*g*-PMMA) during melt mixing, thereby increasing the molecular weight of the PPS composition, which is observed as an increase in the melt viscosity. It was also found that 10 min of mixing time is sufficient to complete the interfacial reaction.

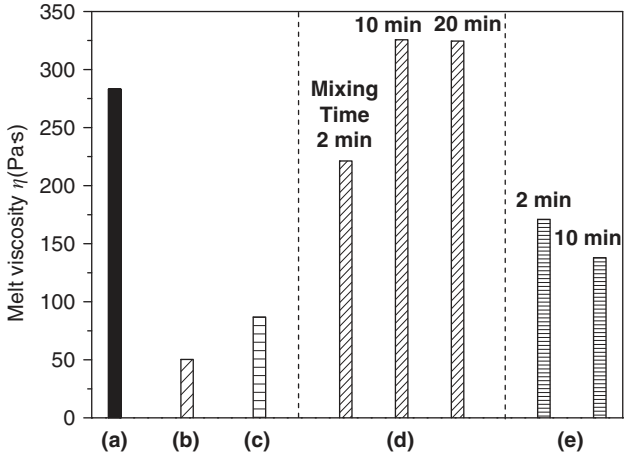

Figure 2 Apparent melt viscosity of (80/20) poly(*p*-phenylene sulfide) (PPS)/poly(ethylene-*ran*-methylacrylate–*ran*-glycidyl methacrylate) (EMA–GMA) and (80/20) PPS/linear low-density polyethylene (LDPE) measured at 300 °C under a flow speed of 100 mm min^{-1}. (**a**) PPS, (**b**) EMA–GMA, (**c**) LDPE, (**d**) (80/20) PPS/EMA–GMA, (**e**) (80/20) PPS/LDPE.

On the other hand, PPS does not react with LDPE so the apparent melt viscosity of PPS/LDPE decreases upon addition of LDPE. Its rheological behavior is similar to that of other immiscible blend systems exhibiting negative deviation from linearity in empirical expressions of viscosity-blend composition relationships and the classical logarithm additivity rule.[32] The reason for this phenomenon is not clear yet, with different possibilities existing, such as interfacial slip between the constituent components and large deformation of the dispersed phase in the continuous phase.

In Figure 3, TEM micrographs of PPS/EMA–GMA, PPS/EGMA-*g*-PMMA and PPS/LDPE at (80/20) weight ratio are shown at two different magnifications. In a non-reactive blend of PPS/LDPE shown in Figure 3c the domain size was as large as 3–5 μm. At higher magnification even crystalline lamellas of LDPE with ca 300 nm in length were observed as white lines. The lamellas in the vicinity of the interface are highly aligned vertically with respect to the interface. This implies that during the cooling process crystallization of molten LDPE is probably initiated at the interface with solidified PPS and then grows vertically from the interface.

On the other hand, in reactive blends of PPS/EMA–GMA and PPS/EGMA-*g*-PMMA shown in Figures 3a and b, the domain size was reduced to sub-micron size, that is, about 0.1 and 0.3 μm, respectively. This significant reduction in the domain size is due to an emulsification effect caused by copolymers formed *in situ* between component polymers at the interface during melt mixing.[33] It is considered that the newly generated copolymers reduce the interfacial tension and suppresses coalescence between domains. In the EMA–GMA domains shown in Figure 3a, lamellas were not observed as clearly as in the LDPE domains implying lower crystallinity of EMA–GMA, as also confirmed by the DSC measurements.

In a literature, it is reported that there are several terminal groups in PPS chains such as –Cl, –SH and –SNa and that some functional groups are also generated as a result of the reaction with *N*-methylpyrrolidone, a solvent used for polymerization of PPS, for example, the *N*-alkylamino group and the amino group.[34] Therefore, it is postulated that the main reaction between PPS and EMA–GMA (or EGMA-*g*-PMMA) occurs between the terminal groups of PPS and the epoxide groups of EMA–GMA engendering a ring-opening reaction. Some other reactions might be also participating at the interface between PPS and EMA–GMA such as a transesterification reaction between the terminal group of PPS and the ester group of EMA–GMA.[10]

Morphology–mechanical property relationships in PPS/EMA–GMA, PPS/EGMA-*g*-PMMA and PPS/LDPE

Next, the mechanical properties of reactive and non-reactive PPS blends were investigated by tensile tests and tensile impact tests. Typical engineering stress-strain curves for various blends at 80/20 weight ratio are shown in Figure 4. It was demonstrated that PPS is inherently very brittle (10% of elongation at break) and has high tensile modulus and strength (1292 MPa and 73 MPa, respectively). Addition of LDPE did not modify the brittleness. On the other hand, addition of 20 wt% of EMA–GMA drastically increased the elongation at break to over 200%, in which the addition of EMA–GMA was more effective than that of EGMA-*g*-PMMA. Detailed values of tensile properties for various blends with different compositions are summarized in Table 2.

In PPS/EMA–GMA blends with different compositions, upon addition of EMA–GMA to PPS up to 20 wt% the elongation at break dramatically increased, however, (70/30) PPS/EMA–GMA showed very poor tensile properties having low elongation at break of 13% as well as low tensile strength and tensile modulus. A TEM micrograph shown in Figure 5a indicated that this is due to a significant increase in the EMA–GMA domain size, in which the substantial amount of copolymers formed at the interface between PPS and EMA–GMA were observed in the EMA–GMA domains in the form of micelles (small white dots with the diameter of <100 nm in the domain).

It is predicted by Leibler[35] that symmetric block copolymers formed at the interface prefer to stay at the interface, whereas asymmetric copolymers tend to move from the interface to the bulk, resulting in the micelle formation. Furthermore, it is observed that a slight deviation from the symmetry and/or the difference in molecular architecture (block or graft) destabilizes the copolymers at the interface.[36,37] In the present study, it is speculated that the reaction between the end group of PPS and the side group of EMA–GMA results in copolymers having a comb-like architecture, in which the teeth of the comb are composed of the PPS block in the matrix. Therefore, it is surmised that the asymmetric copolymers are destabilized at the interface. In addition, a significant reduction of the interfacial tension upon the sufficient amount of copolymer formation facilitates the removal of copolymers from the interface, resulting in the newly exposed interface without being covered by the copolymers. Consequently, the interfacial reaction continuously generates more copolymers at the interface. The inclusion of the micelles apparently increases the melt viscosity of the domains, which consequently prevents a fine distribution of the domains.

By contrast, in PPS/EGMA-*g*-PMMA blends containing 10–30 wt% of EGMA-*g*-PMMA, (70/30) PPS/EGMA-*g*-PMMA showed extremely high elongation at break of over 300%, which had a similar morphology to (80/20) PPS/EGMA-*g*-PMMA. Figures 3b and 5b indicate that the EGMA-*g*-PMMA domain size in (70/30) PPS/EGMA-*g*-PMMA is only slightly larger than that in the (80/20) blend. It is interesting to find in the (70/30) PPS/EGMA-*g*-PMMA blends that grafting the PMMA block to the EGMA main chains in EGMA-*g*-PMMA prevents pull-out of the copolymers formed *in situ* at the interface to the EGMA-*g*-PMMA domains, when Figure 5b was compared with Figure 5a. This is most likely because the PMMA grafts prevent the PPS terminal groups from reacting with the epoxide groups located in

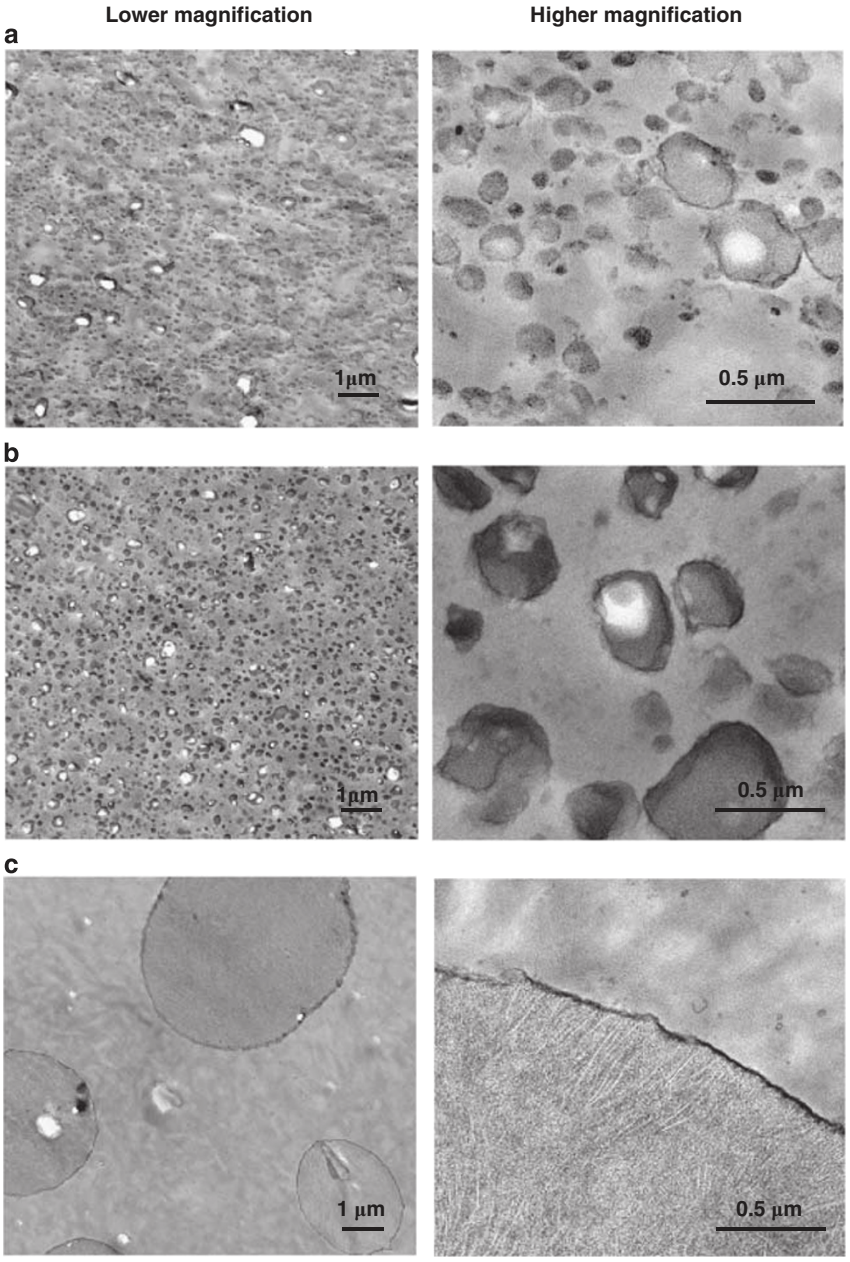

Figure 3 Transmission electron microscopy micrographs of (**a**) (80/20) poly(*p*-phenylene sulfide) (PPS)/poly(ethylene-*ran*-methylacrylate–*ran*-glycidyl methacrylate), (**b**) (80/20) PPS/poly(ethylene-*ran*-glycidyl methacrylate)-*graft*-poly(methyl methacrylate) and (**c**) (80/20) PPS/linear low-density polyethylene stained by RuO_4.

the main chain, thereby decreasing the interfacial tension to less extent and suppressing the pull-out of *in situ* formed copolymers.

Figure 6 shows effects of addition of EMA–GMA (or EGMA-*g*-PMMA, LDPE) to PPS on tensile impact strength of their PPS blends. Here, it was demonstrated that addition of EMA–GMA (or EGMA-*g*-PMMA) increases the tensile impact strength, however, the micelle formation by the *in situ* formed copolymers observed in (70/30) PPS/EMA–GMA results in a significant decrease in the tensile impact strength. Taking morphology into consideration as reported in Figure 5, these results indicate that incorporation of a large amount of EMA–GMA does not necessarily result in an increase of impact strength and that the good dispersion of the EMA–GMA domains is essential.

The tensile impact strength of the blends is greatly dependent upon the dissipation capacity of the impact energy through the matrix and delivery of the internal stress of the continuous phase to the dispersed phase. A comparison between PPS/EMA–GMA (or PPS/EGMA-*g*-PMMA) and PPS/LDPE clearly demonstrated that the copolymers formed *in situ* function very effectively for this energy dissipation capacity. It is reported in the literature that in a study of PPS mixed with 0–20 wt% of poly(ethylene-*stat*-glycidyl methacrylate)-*graft*-poly(acrylonitrile-*stat*-styrene) (EGMA-*graft*-SAN) 5 wt% of EGMA-*graft*-SAN inclusion exhibited higher mechanical properties than any other compositions at 25 °C.[28] In the same paper, morphology was investigated by polarized optical microscopy, in which the observation of morphology including micelle formation or submicron size

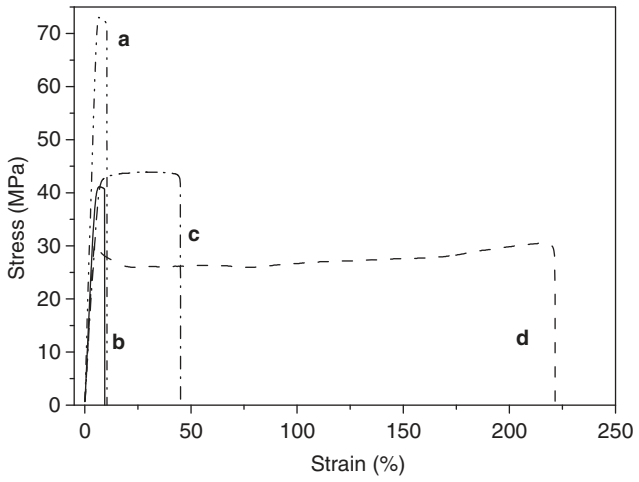

Figure 4 Engineering stress-strain curves of poly(*p*-phenylene sulfide) (PPS), poly(ethylene-*ran*-methylacrylate–*ran*-glycidyl methacrylate) (EMA–GMA), linear low-density polyethylene (LDPE) and PPS blends. (**a**) PPS, (**b**) (80/20) PPS/LDPE, (**c**) (80/20) PPS/EGMA-*g*-PMMA, (**d**) (80/20) PPS/EMA–GMA.

Table 2 Mechanical properties of various PPS blends and their component polymers

PPS	EMA–GMA	EGMA-*g*-PMMA	LDPE	Tensile properties			Impact strength
(wt%)	(wt%)	(wt%)	(wt%)	TM (MPa)	TS (MPa)	EB (%)	IS (kJ m^{-2})
100	0	0	0	1292	73	10	89
0	100	0	0	6	3	519	615
0	0	100	0	—	—	—	—
0	0	0	100	78	14	839	NB
80	20	0	0	802	36	221	300
80	0	20	0	698	44	45	141
80	0	0	20	868	41	9	—
90	10	0	0	945	43	188	204
80	20	0	0	802	36	221	300
70	30	0	0	220	13	13	165
90	0	10	0	757	58	22	77
80	0	20	0	698	44	45	141
70	0	30	0	548	44	312	441

Abbreviations: EB, elongation at break; EMA–GMA, poly(ethylene-*ran*-methylacrylate–*ran*-glycidyl methacrylate); EGMA-*g*-PMMA, poly(ethylene-*ran*-glycidyl methacrylate)-*graft*-poly(methyl methacrylate); IS, tensile impact strength; LDPE, linear low-density polyethylene; NB, non-breakable; TM, tensile modulus; TS, tensile strength.

distribution shown in Figure 5 is impossible. So it is reported in the paper that the domain size of EGMA-*graft*-SAN increased from ca 1.25–2.75 μm as an increase of EGMA-*graft*-SAN content from 2 to 20 wt%. The present PPS/EMA–GMA has domain size about 1/20 smaller when compared with their system at 80/20 weight ratio, which is most likely due to the sample preparation at high shear rate. In their study on PPS/EGMA-*graft*-SAN the values of the elongation at break hardly changed despite the addition of EGMA-*graft*-SAN, remaining a few %, whereas in this study it increased dramatically. Furthermore, in their study the tensile modulus monotonically decreased with increase of EGMA-*graft*-SAN content, in which about 33% of reduction was observed at 20 wt% of EGMA-*graft*-SAN content. The same degree of reduction in tensile modulus was also observed in our PPS/EMA–GMA. In their notched Izod impact test, the impact strength increased

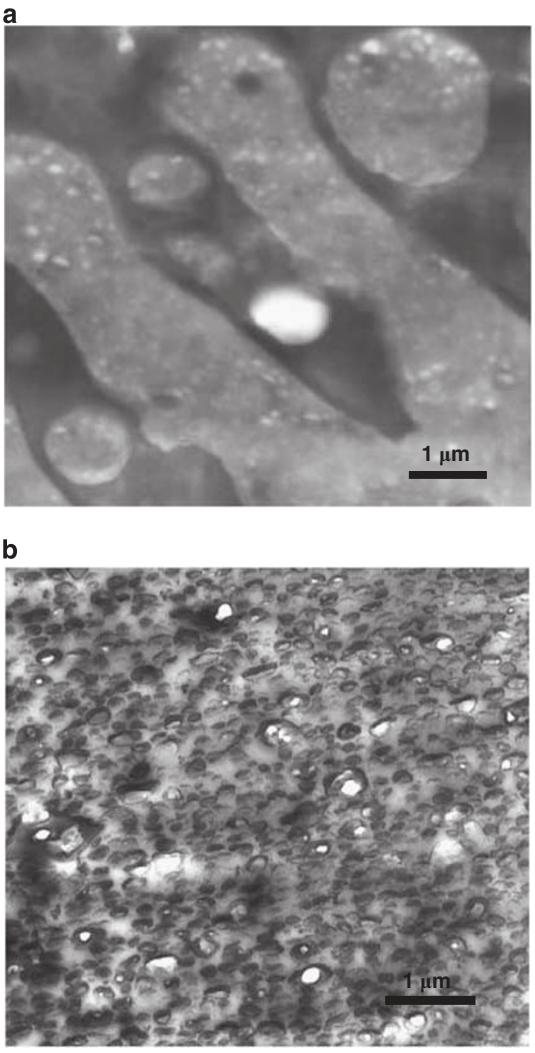

Figure 5 Transmission electron microscopy micrographs of (**a**) (70/30) poly(*p*-phenylene sulfide) (PPS)/poly(ethylene-*ran*-methylacrylate–*ran*-glycidyl methacrylate) and (**b**) (70/30) PPS/poly(ethylene-*ran*-glycidyl methacrylate)-*graft*-poly(methyl methacrylate) stained by RuO_4.

from 1.7 to 2.4 kgcm cm^{-1} upon addition of 20 wt% of EGMA-*graft*-SAN, which corresponds to a 41% increase compared with that of pristine PPS. Interestingly, the impact strength became the highest at 5 wt% of the EGMA-*graft*-SAN content, in which the extent of increase was 72%. It was explained that smaller size and even distribution of the domains could effectively distribute the impact energy, although the fracture surface of this PPS alloy did not differ from that of pristine PPS. In our study, addition of 20 wt% of EMA–GMA and EGMA-*g*-PMMA increased the impact strength by 237 and 58%, respectively, compared with that of pristine PPS so that both reactive polymers are more effective for toughening when compared with the best value in EGMA-*graft*-SAN. It was also demonstrated in this study that large domains formed as a result of an increase in melt viscosity of the domains by inclusion of the substantial amount of micelles significantly deteriorates toughness, as observed in (70/30) PPS/EMA–GMA.

It was also attempted to blend reactive ethylene copolymer containing about 2 wt% of maleic anhydride and PPS chemically treated with diphenylmethane diisocyanate in an extruder before the melt blending.[27] Scanning electron microscopy measurements showed that the resultant blend composed of (80/20) so-modified PPS and the

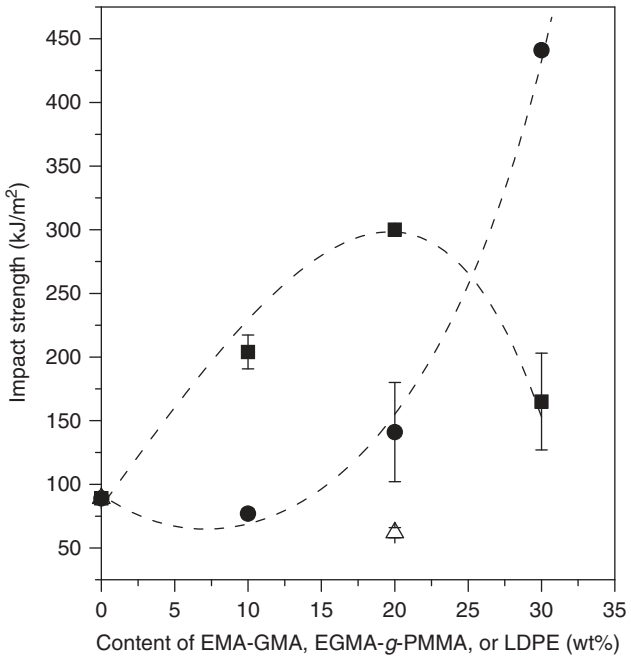

Figure 6 Effect of addition of poly(ethylene-*ran*-methylacrylate–*ran*-glycidyl methacrylate) (EMA–GMA), poly(ethylene-*ran*-glycidyl methacrylate)-*graft*-poly(methyl methacrylate) (EGMA-*g*-PMMA) and linear low-density polyethylene (LDPE) on tensile impact strength of their PPS blends. The bar indicates the s.d. ■: PPS/EMA–GMA, ●: PPS/EGMA-*g*-PMMA, △: PPS/LDPE.

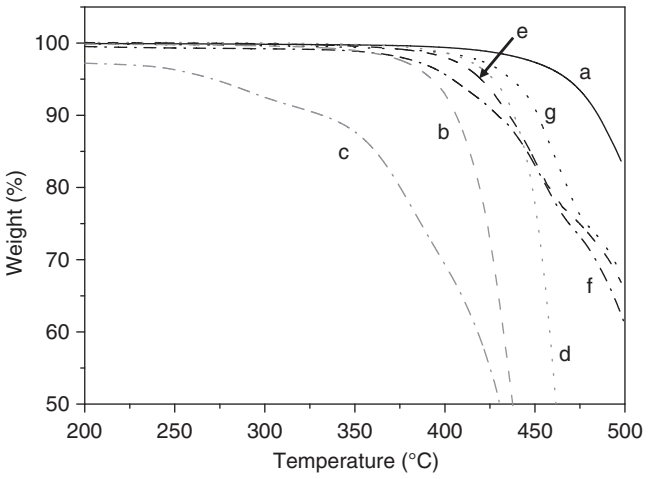

Figure 7 Thermogravimetric analysis curves of poly(*p*-phenylene sulfide) (PPS), poly(ethylene-*ran*-methylacrylate–*ran*-glycidyl methacrylate) (EMA–GMA), linear low-density polyethylene (LDPE) and various PPS blends measured in N_2. (**a**) — PPS, (**b**) – – – EMA–GMA, (**c**) –·–·– EGMA-*g*-PMMA, (**d**) ····· LDPE, (**e**) - - - (80/20) PPS/EMA–GMA, (**f**) - · - · (80/20) PPS/EGMA-*g*-PMMA, (**g**) ····· (80/20) PPS/LDPE.

ethylene copolymer had an average domain size of 0.25 μm, whereas the blend prepared using unmodified (conventional) PPS had an average domain size of 1 μm. Their critical surface-to-surface interparticle distance, τ_c, was estimated to be about 0.1 μm. This value of τ_c roughly corresponds to a domain size of 0.2 μm for the 80/20 blends according to the equation they used:

$$\tau = d\{(\pi/6\phi_d)^{1/3} - 1\} \quad (3)$$

where τ, d, and ϕ_d are surface-to-surface interparticle distance, domain size and volume fraction of the domain, respectively. The TEM micrographs for our (80/20) PPS/EMA–GMA and PPS/EGMA-*g*-PMMA shown in Figure 3, demonstrate that the former blend has a smaller surface-to-surface interparticle distance than the critical value of 0.1 μm, whereas the latter has close to this value or even slightly larger. Therefore, the former PPS/EMA–GMA might manifest higher impact strength than the latter because of its smaller τ value, although a difference in mechanical properties between EMA–GMA and EGMA-*g*-PMMA might also partly affect.

In another study[10] of a non-reactive blend of PPS/aromatic thermotropic LCP, when compared with pristine PPS, (75/25) PPS/LCP blend had lower Izod impact strength in the unnotched tests, however, (75/25) PPS/LCP blend compatibilized by 2.5 wt% of dicarboxyl-terminated PPS had higher impact strength by ca 1.5 times. The present results shown in Figure 6 imply that the addition of EMA–GMA (or EGMA-*g*-PMMA) is more effective in the enhancement of impact strength of PPS blends.

Thermal properties of PPS/EMA–GMA, PPS/EGMA-*g*-PMMA, and PPS/LDPE

The thermal stability of the PPS/EMA–GMA and PPS/EGMA-*g*-PMMA melt-mixed blends was investigated using thermogravimetric analysis in a nitrogen atmosphere, and the results are shown in Figure 7. It was found that pristine EGMA-*g*-PMMA is less stable during heating when compared with pristine EMA–GMA, suggesting that the thermal decomposition is initiated in the PMMA block. It is reported that pristine PMMA is degraded by end-chain scission, which is followed by random scission giving monomers as products.[38,39] Therefore, the (80/20) PPS/EGMA-*g*-PMMA rapidly lost weight above 350 °C although the (80/20) PPS/EMA–GMA was thermally stable up to about 400 °C.

Table 3 summarizes the results of thermal decomposition for various blends, in which the onset temperature of decomposition observed at 5 wt% loss (defined as the decomposition temperature in this paper) and the residual remaining weight after a specimen was heated up to 500 °C are shown. The incorporation of 20 wt% of EMA–GMA and EGMA-*g*-PMMA to PPS decreased the decomposition temperature by 44 and 59 °C, respectively. Although pristine EGMA-*g*-PMMA had a decomposition temperature that is 120 °C lower than pristine EMA–GMA, the (80/20) PPS/EGMA-*g*-PMMA blend had a decomposition temperature just 15 °C lower than the PPS/EMA–GMA sample at the same composition. This implies that surrounding the EGMA-*g*-PMMA by the PPS matrix with high thermal stability efficiently protects the EGMA-*g*-PMMA domain from thermal degradation. Table 3 also indicates that the thermal stability of the (80/20) PPS/EMA–GMA and PPS/EGMA-*g*-PMMA blends is quite high, retaining a decomposition temperature above 400 °C.

It is reported in the literature that no thermal decomposition occurs in polyethylene grafted with GMA in a nitrogen atmosphere until 300 °C whereas the decomposition of polyethylene grafted with acrylic acid occurs below 250 °C.[16] This result indicates that the GMA group used for the present study is suitable for a process of producing the high performance engineering plastic blends.

In summary, it has been demonstrated that the drawbacks of PPS's brittleness and low toughness can be solved by blending PPS with reactive ethylene copolymers. Compared with other PPS blends reported in the literature, the present blends have much smaller domains that give higher ductility and toughness. These small domains probably arose from high shear rate used for the sample

Table 3 Thermal decomposition of various PPS blends and their component polymers measured by TGA in nitrogen atmosphere

PPS	*EMA–GMA*	*EGMA-g-PMMA*	*LDPE*	*Thermal decomposition*	
(wt%)	*(wt%)*	*(wt%)*	*(wt%)*	*Decomposition temperature (°C)*[a]	*Residue (wt%)*[b]
100	0	0	0	463	79
0	100	0	0	393	0
0	0	100	0	271	0
0	0	0	100	427	0
80	20	0	0	419	67
80	0	20	0	404	61
80	0	0	20	438	68
90	10	0	0	428	74
80	20	0	0	419	67
70	30	0	0	413	58
90	0	10	0	423	72
80	0	20	0	404	61
70	0	30	0	397	56

Abbreviations: EMA–GMA, poly(ethylene-*ran*-methylacrylate–*ran*-glycidyl methacrylate); EGMA-*g*-PMMA, poly(ethylene-*ran*-glycidyl methacrylate)-*graft*-poly(methyl methacrylate); LDPE, linear low-density polyethylene; TGA, thermogravimetric analysis.
[a]Temperatures observed at 5% weight loss.
[b]Remaining weight after heating to 500 °C in N_2.

preparation. It was indicated that smaller domain size and good domain distribution are essential to manifest superior mechanical properties. The obtained reactive PPS blends also showed good thermal stability close to 400 °C. Although it has been believed that it is very difficult to melt mix polymeric materials with a difference in T_m over 200 °C, this work demonstrated that it was possible. In this manner, the toughening of a super-engineering plastic, PPS, was successfully carried out.

CONCLUSIONS

The present work on PPS/EMA–GMA and PPS/EGMA-*g*-PMMA allowed the following important conclusions:

(1) The reactive PPS blends, (80/20) PPS/EMA–GMA and PPS/EGMA-*g*-PMMA, prepared under an extremely high shear rate have significantly smaller domain size and good domain distributions, and manifest superior mechanical properties in tensile and impact tests compared with pristine PPS.
(2) In the (70/30) PPS/EMA–GMA blend, micelles were formed as a result of the pulling out of the *in situ* formed copolymers from the interface to the inside of the EMA–GMA domains. The inclusion of micelles obviously increases the melt viscosity of the domains so that a fine distribution of the domains is prevented. Therefore, mechanical properties were significantly deteriorated, lowering ductility and toughness.
(3) The obtained reactive PPS blends showed good thermal stability up to 400 °C.
(4) In a comparison between PPS/EMA–GMA and PPS/EGMA-*g*-PMMA, the former blend showed better mechanical properties and thermal stability than the latter.

CONFLICT OF INTEREST

The authors declare no conflict of interest.

ACKNOWLEDGEMENTS

Financial supports were kindly provided by Grant-in-Aid for Scientific Research and the Frontier Project supported by the Ministry of Education, Culture, Sports, Science and Technology of Japan.

1 Masamoto, J. Poly(p-phenylene sulfide), In: *Polymer Data Handbook* (ed. Mark, J.E.) 714–721 (Oxford University Press, 1999).
2 López, L. C., Wilkes, G. L. & Geibel, J. Crystallization kinetics of poly(*p*-phenylene sulphide): the effect of branching agent content and endgroup counter-atom. *Polymer* **30,** 147–155 (1989).
3 Menczel, J. D. & Collins, G. L. Thermal analysis of poly(phenylene sulfide) polymers. I: thermal characterization of PPS polymers of different molecular weights. *Polym. Eng. Sci.* **32,** 1264–1269 (1992).
4 Hill Jr, H. W. & Brady, D. G. in *Encyclopedia of Polymer Science and Technology*, vol. 11, 2nd edn (ed. Mark, H.F.) 531 (Wiley-Interscience, New York, 1988).
5 Cheung, M. F. & Plummer, H. K. Tensile fracture morphology of polysulfone-poly(phenylene sulfide) blends. *Polym. Bull.* **26,** 349–356 (1991).
6 Shibata, M., Yosomiya, R., Jiang, Z., Yang, Z., Wang, G., Ma, R. & Wu, Z. Crystallization and melting behavior of poly(*p*-phenylene sulfide) in blends with poly(ether sulfone). *J. Appl. Polym. Sci.* **74,** 1686–1692 (1999).
7 Lai, M. & Liu, J. Thermal and dynamic mechanical properties of PES/PPS blends. *J. Therm. Anal. Cal.* **77,** 935–945 (2004).
8 Gabellini, G., de Moraes, M. B. & Bretas, R. E. S. Poly(*p*-phenylene sulphide)/liquid crystalline polymer blends. I. Miscibility and morphologic studies. *J. Appl. Polym. Sci.* **60,** 21–27 (1996).
9 Gopakumar, T. G., Ghadage, R. S., Ponrathnam, S., Rajan, C. R. & Fradet, A. Poly(phenylene sulfide)/liquid crystalline polymer blends: 1. Non-isothermal crystallization kinetics. *Polymer* **38,** 2209–2214 (1997).
10 Gopakumar, T. G., Ponrathnam, S., Lele, A. & Fradet, A. *In situ* compatibilisation of poly(phenylene sulphide)/wholly aromatic thermotropic liquid crystalline polymer blends by reactive extrusion: morphology, thermal and mechanical properties. *Polymer* **40,** 357–364 (1999).
11 Tang, W., Hu, X., Tang, J. & Jin, R. Toughening and compatibilization of polyphenylene sulfide/nylon 66 blends with SEBS and maleic anhydride grafted SEBS triblock copolymers. *J. Appl. Polym. Sci.* **106,** 2648–2655 (2007).
12 Zhang, R., Huang, Y., Min, M., Gao, Y., Lu, A. & Lu, Z. Nonisothermal crystallization of polyamide 66/poly(phenylene sulfide) blends. *J. Appl. Polym. Sci.* **107,** 2600–2606 (2008).
13 An, J. B., Suzuki, T., Ougizawa, T., Inoue, T., Mitamura, K. & Kawanishi, K. Studies on miscibility and phase-separated morphology of nylon 4,6/poly(phenylene sulfide) blend under shear flow. *J. Macromol. Sci., Physics B* **41,** 407–418 (2002).
14 Jog, J. P., Shingankuli, V. L. & Nadkarni, V. M. Crystallization of poly(phenylene sulfide) in blends with high density polyethylene and poly(ethylene terephthalate). *Polymer* **34,** 1966 (1993).
15 Hanley, S. J., Nesheiwat, A. M., Chen, R. T., Jamieson, M., Pearson, R. A. & Sperling, L. H. Phase separation in semicrystalline blends of poly(phenylene sulfide) and poly(ethylene terephthalate). II. Effect of poly(phenylene sulfide) homopolymer solubilization of PPS-graft-PET copolymer on morphology and crystallization behavior. *J. Polym. Sci., Part B: Polym. Phys.* **38,** 599–610 (2000).
16 Chen, C. M., Hsieh, T. E. & Liu, M. O. Preparation of epoxy-modified polyethylene by graft extrusion and its applications to polyphenylene sulfide alloys as a compatibilizer. *React. Funct. Polym.* **68,** 1307–1313 (2008).
17 Kubo, K. & Masamoto, J. Microdispersion of polyphenylene ether in polyphenylene sulfide/polyphenylene ether alloy compatibilized by styrene-*co*-glycidyl methacrylate. *J. Appl. Polym. Sci.* **86,** 3030–3034 (2002).
18 Choi, J., Lim, S., Kim, J. & Choe, C. R. Studies of an epoxy-compatibilized poly(phenylene sulfide)/polycarbonate blend. *Polymer* **38,** 4401–4406 (1997).

19 Mizuno, S. & Kawabata, J. Poly(phenylene sulfide) alloys in *Development and Application of Polymer Alloys* (eds. Akiyama, S., Izawa, S.), Chapter 14 (CMC Co., Ltd, Tokyo, Japan, 2003).
20 Chen, Z., Liu, X., Li, T. & Lü, R. Mechanical and tribological properties of PA66/PPS blend. II. Filled with PTFE. *J. Appl. Polym. Sci.* **101,** 969–977 (2006).
21 Chen, Z., Liu, X., Lü, R. & Li, T. Mechanical and tribological properties of PA66/PPS blend. III. Reinforced with GF. *J. Appl. Polym. Sci.* **102,** 523–529 (2006).
22 Zou, H., Wang, K., Zhang, Q. & Fu, Q. A change of phase morphology in poly(*p*-phenylene sulfide)/polyamide 66 blends induced by adding multi-walled carbon nanotubes. *Polymer* **47,** 7821–7826 (2006).
23 Yoon, P. J. & White, J. L. Interfacial tension of poly(*p*-phenylene sulfide) with other polymer melts. *J. Appl. Polym. Sci.* **51,** 1515–1519 (1994).
24 Chen, T. H. & Su, A. C. Morphology of poly(p-phenylene sulfide) polyethylene blends. *Polymer* **34,** 4826–4831 (1993).
25 Hisamatsu, T., Nakano, S., Adachi, T., Ishikawa, M. & Iwakura, K. The effect of compatibility on toughness of PPS/SEBS polymer alloy. *Polymer* **41,** 4803–4809 (2000).
26 Hwang, S. H., Kim, M. J. & Jung, J. C. Mechanical and thermal properties of syndiotactic polystyrene blends with poly(*p*-phenylene sulfide). *Eur. Polym. J.* **38,** 1881–1885 (2002).
27 Masamoto, J. & Kubo, K. Elastomer-toughened poly(phenylene sulfide). *Polym. Eng. Sci.* **36,** 265–270 (1996).
28 Lee, S. & Chun, B. C. Effect of EGMA content on the tensile and impact properties of poly(phenylene sulfide)/EGMA blends. *Polymer* **39,** 6441–6447 (1998).
29 Takase, H., Mikata, Y., Matsuda, S. & Murakami, A. Dispersion of carbon-nanotubes in a polymer matrix by a twin-screw extruder. *Seikei-Kakou* **14,** 126–131 (2002).
30 Oyama, H. T., Sekikawa, M. & Ikezawa, Y. Influence of the polymer/inorganic filler interface on the mechanical, thermal, and flame retardant properties of polypropylene/magnesium hydroxide composites. *J. Macromol. Sci., Part B: Phys* **50,** 463–483 (2011).
31 Liang, J. Z. & Li, R. K. Y. Rheological properties of glass bead-filled low-density polyethylene composite melts in capillary extrusion. *J. Appl. Polym. Sci.* **73,** 1451–1456 (1999).
32 Lee, B. L. & White, J. L. Experimental studies of disperse 2-phase flow of molten polymers through dies. *Trans. Soc. Rheol.* **19,** 481–492 (1975).
33 Macosko, C. W. Morphology development and control in immiscible polymer blends. *Macromol. Symp.* **149,** 171–184 (2000).
34 Wade, B., Sbhiraman, A. S., Wharry, S. & Sutherlin, D. High-temperature, high-resolution nuclear magnetic resonance of poly(*p*-phenylene sulfide). *J. Polym. Sci., Part B: Polym. Phys.* **28,** 1233–1249 (1990).
35 Leibler, L. Emulsifying effects of block copolymers in incompatible polymer blends. *Makromol. Chem. Macromol. Symp.* **16,** 1–17 (1988).
36 Ibuki, J., Charoensirisomboon, P., Chiba, T., Ougizawa, T., Inoue, T., Weber, M. & Koch, E. Reactive blending of polysulfone with polyamide: a potential for solvent-free preparation of the block copolymer. *Polymer* **40,** 647–653 (1999).
37 Charoensirisomboon, P., Inoue, T. & Weber, M. Pull-out of copolymer *in situ*-formed during reactive blending: effect of the copolymer architecture. *Polymer* **41,** 6907–6912 (2000).
38 Manring, L. E. Thermal degradation of saturated poly(methyl methacrylate). *Maromolecules* **21,** 528–530 (1988).
39 Ahmad, Z., Al-Awadi, N. A. & Al-Sagheer, F. Thermal degradation studies in poly(vinyl chloride)/poly(methyl methacrylate) blends. *Polym. Degrad. Stab.* **93,** 456–465 (2008).